Cancer Management and Research

Dovepress

open access to scientific and medical research

Open Access Full Text Article

ORIGINAL RESEARCH

Long Non-Coding RNA UBA6-AS1 Promotes the Malignant Properties of Glioblastoma by Competitively Binding to microRNA-760 and Enhancing Homeobox A2 Expression

This article was published in the following Dove Press journal:
Cancer Management and Research

Feifei Cheng[1]
Jiang Liu[1]
Yundong Zhang[1]
Qiuxiang You[1]
Bo Chen[2]
Jing Cheng[1]
Chunyan Deng[1]

[1]Department of Neurology, The Third Affiliated Hospital of Chongqing Medical University, Chongqing 401120, People's Republic of China; [2]Department of Pharmacology, College of Pharmacy, Chongqing Medical University, Chongqing 401120, People's Republic of China

Background: The dysregulation of long non-coding RNAs is a frequent finding in glioblastoma (GBM) and is considered as a crucial mechanism contributing to GBM oncogenesis and progression. The biological roles and underlying mechanisms of action of UBA6 antisense RNA 1 (UBA6-AS1) in GBM have been rarely investigated. Therefore, the aim of the present study was to investigate in detail the role of UBA6-AS1 in the modulation of the malignant properties of GBM and explore the possible underlying mechanism(s).

Methods: The expression of UBA6-AS1 in GBM was determined via reverse transcription-quantitative PCR. Cell Counting Kit-8 assay, flow cytometric analysis, Transwell migration and invasion assays, and in vivo tumorigenicity assay were applied to elucidate the biological effects of UBA6-AS1 on GBM cells. The possible biological events associated with UBA6-AS1 were investigated by luciferase reporter, RNA immunoprecipitation (RIP) and rescue assays.

Results: UBA6-AS1 was overexpressed in GBM, which was consistent with the data from The Cancer Genome Atlas database. In the case of UBA6-AS1 depletion, GBM cell proliferation, migration and invasion were notably decreased and cell apoptosis was enhanced in vitro. Additionally, knockdown of UBA6-AS1 suppressed the proliferation of GBM cells in vivo. Mechanistically, UBA6-AS1 functioned as a competing endogenous RNA by adsorbing miR-760 and, consequently, upregulating homeobox A2 (HOXA2) expression. Rescue experiments demonstrated that the UBA6-AS1 silencing-mediated regulatory effects on GBM cells were reversed by the decrease of miR-760 or restoration of HOXA2 expression.

Conclusion: Therefore, the results of the present study revealed that UBA6-AS1 promoted the malignant progression of GBM via targeting the miR-760/HOXA2 axis, thereby representing a promising effective target for the treatment of GBM.

Keywords: UBA6 antisense RNA 1, long non-coding RNA, homeobox A2, glioblastoma

Introduction

Glioma is the secondary malignant tumor of the central nervous system.[1] The World Health Organization (WHO)[2] classifies glioma into four subtypes, including low-grade astrocytoma (grades I–II), anaplastic astrocytoma (grade III) and glioblastoma multiforme (GBM; WHO grade IV). GBM is the most aggressive and lethal among all brain tumors, and it is characterized by unlimited growth, infiltration,

Correspondence: Chunyan Deng
Email dcycq_2008@163.com

high incidence of recurrence, resistance to chemotherapy.[3,4] With the development of medical technology, multiple treatment techniques, including surgery, radiotherapy, chemotherapy, immunotherapy and targeted therapies, have been employed to treat patients with GBM, and have managed to prolong the survival and improve the quality of life of the patients;[5] however, GBM remains incurable, with a 5-year survival rate of only 5% globally.[6,7] Gliomagenesis and tumor development are complicated processes that have yet to be fully elucidated.[8,9] Thus, it is crucial to fully elucidate GBM pathogenesis and identify effective targets for diagnosis and anticancer therapy.

Long non-coding RNAs (lncRNAs) are a group of RNA transcripts that exceed 200 nucleotides in length.[10] They lack protein-coding ability, but are implicated in the regulation of gene expression at different levels, including the epigenetic, transcriptional and post-transcriptional levels.[11] LncRNAs are confirmed as fine-tuners and regulators of physiological and pathological behaviors.[12] Extensive studies have demonstrated that lncRNAs play a key role in regulating the cancer development and progression.[13–15] In recent years, authoritative research has uncovered the aberrant expression of lncRNAs in GBM and validated lncRNAs as promoters or inhibitors of cancer-associated processes.[16–18]

Similar to lncRNAs, microRNAs (miRNAs) comprise another class of single-stranded, non-coding RNA transcripts, with a length ranging from 22 to 24 nucleotides.[19] miRNAs may directly interact with the 3′-untranslated region (3′-UTR) of target genes and inhibit their expression, consequently causing mRNA degradation or translation inhibition.[20] A novel regulatory mechanism, referred to as the competing endogenous RNA (ceRNA) theory, was recently proposed and has been attracting considerable attention.[21,22] lncRNAs can adsorb or sponge certain miRNAs, thus decreasing the miRNA-mediated mRNA inhibition.[23] Accordingly, an in-depth investigation of the lncRNAs and miRNAs involved in GBM is required, which may provide novel insight into GBM oncogenesis and progression.

The aberrant expression of lncRNAs is a frequent occurrence in GBM and has been considered as a crucial mechanism contributing to GBM oncogenesis and progression.[24,25] By searching The Cancer Genome Atlas (TCGA) database, plenty of lncRNAs was differentially expressed in GBM. Among them, UBA6 antisense RNA 1 (UBA6-AS1) is one of the most overexpressed lncRNAs. Furthermore, the expression, function and possible mechanism of action of UBA6 antisense RNA 1 (UBA6-AS1) in GBM have not been investigated to date. Therefore, the aim of the present study was to evaluate the biological effects of UBA6-AS1 on GBM and elucidate the associated mechanisms.

Materials and Methods

Tissues and Cell Lines

The present study was performed following approval provided by the Ethics Committee of the Third Affiliated Hospital of Chongqing Medical University (EC. TAHCMU-2016.0411) and was conducted in all accordance with the principles outlined in the World Medical Association Declaration of Helsinki. Written informed consents were obtained from all participants. A total of 49 GBM tissues were obtained from patients with GBM admitted to the Third Affiliated Hospital of Chongqing Medical University. Furthermore, normal brain tissue samples were collected from 13 patients suffering from craniocerebral injury and undergoing brain tissue resection. None of these participants had received chemotherapy, radiotherapy or other anticancer treatments prior to surgical excision. The resected tissues were immediately immersed in liquid nitrogen and stored until further use.

The GBM cell lines A172 and U251 were purchased from the Shanghai Institutes for Biological Sciences Cell Resource Center (Shanghai, China) and cultured in DMEM (Gibco; Thermo Fisher Scientific, Inc.) supplemented with 10% FBS (Gibco, Thermo Fisher Scientific, Inc.). The U138 and T98 GBM cell lines were obtained from the American Type Culture Collection. Cell culture medium was composed of 90% Minimum Essential Medium (Gibco; Thermo Fisher Scientific, Inc.) and 10% FBS. NHA, a normal human astrocyte cell line, was obtained from ScienCell Research Laboratories (Carlsbad, CA, USA) and cultured in astrocyte medium (ScienCell Research Laboratories). All the cell lines were grown in a humidified incubator at 37°C with 5% CO_2.

Small Interfering RNAs (siRNAs), Plasmids, miRNA Mimic/Inhibitor and Cell Transfections

UBA6-AS1 silencing was implemented by transfecting small interfering RNA (siRNA) targeting UBA6-AS1 (si-UBA6-AS1; Shanghai GenePharma, Co., Ltd.). Negative control (NC) siRNA (si-NC; Shanghai GenePharma, Co.,

Ltd.) served as the control for si-UBA6-AS1. The upregulation and downregulation of miR-760 expression were performed by transfecting miR-760 mimic and miR-760 inhibitor, respectively (Sangon Biotech Co., Ltd.). NC miRNA mimic (miR-NC) and NC inhibitor were used as the controls for miR-760 mimic and miR-760 inhibitor, respectively. The full length of HOXA2 was amplified and inserted into the pcDNA3.1 plasmid, producing the overexpression plasmids pcDNA3.1-HOXA2. Cells were seeded into 6-well plates, and all oligonucleotides and plasmids were transfected into cells using Lipofectamine™ 2000 reagent (Invitrogen; Thermo Fisher Scientific, Inc.) according to the manufacturer's instructions.

Reverse Transcription-Quantitative PCR (RT-qPCR) Analysis

Total RNA was extracted using TRIzol® reagent (Invitrogen; Thermo Fisher Scientific, Inc.) according to the manufacturer's instructions. For detection of miR-760, total RNA was reverse-transcribed into complementary DNA using the miRcute miRNA First-Strand cDNA Synthesis Kit (Tiangen Biotech), whi... miRcute miRNA qPCR Detection Kit SYBR G...een (Tiangen Biotech) was employed for cond...ing qP... U6 small nuclear RNA served as hous...keeping gene f... miR-760. For the quantification o... UBA... and HOXA2, cDNA was generated ...y using ...rimeScript™ RT reagent kit with gDNA E... (Takara B...echnology Co., Ltd.). Using cDNA as the ...mplate, TB Green® Premix Ex Taq™ II ...akara Biotec...ology Co., Ltd.) was employed to carry ...t qPCR. UBA6-AS1 and HOXA2 levels we... no...alized based on GAPDH. All data were n...lized ...ing th... $2^{-\Delta\Delta Cq}$ method.

Cell C...ting Kit-8 (CCK-8) Assay

The transfe...d GBM cells were harvested at 24 h post-transfection and ...dded to 96-well plates at a density of 2000 cells/well. Cell proliferation was measured by the CCK-8 assay (Beyotime Institute of Biotechnology) at 0, 1, 2 and 3 days after cell transfection. Briefly, 10 µL CCK-8 reagent was added to each well of the 96-well plates, and an additional 2-h incubation was performed at 37°C with 5% CO_2. Finally, the absorbance value was determined using a microplate reader (Bio-Rad Laboratories, Inc.) at a wavelength of 450 nm.

Flow Cytometric Analysis

After 48 h, transfected GBM cells were detached with ethylene diamine tetraacetic acid-free trypsin and stored in the flow tubes. Cell apoptosis was analyzed with the Annexin V-FITC Apoptosis Detection Kit (Beyotime Institute of Biotechnology). Following centrifugation at 1000 x g for 5 min, the supernatant fluid was discarded, and the cells were resuspended in Annexin V-FITC binding buffer, followed by double staining with 5 µL Annexin V-FITC and 10 µL PI. After 20 min of culture at room temperature in the dark, flow cyto... (BD Biosciences) was applied to determine apo...osis.

Transwell Migra...on and ...vasi...n Assays

Cell migration a... invasi... abilities ...were detected via Transwell ass... (8-p... ...ter; BD ...Biosciences). For the migration a...y, $5x10^4$ t...nsfe...d GBM cells resuspended in 200 ... cu...re medium ...ithout FBS were inoculated into the top cha...ers; the bottom chambers were filled ...th 500 µL culture ...edium supplemented with 20% FBS. ...ollowing c...ture for 1 day, the non-migrating cells were ...moved wit... a cotton swab, whereas the cells migrating th...h th... membrane were fixed with methanol and ...tained with 0.1% crystal violet solution. The migrating cells were examined and counted under a light microscope (Olympus Corporation). For the invasion assay, the same number of transfected GBM cells was seeded into the top chambers that were precoated with Matrigel solution (BD Diagnostics), and the following experimental procedures were as described for the migration assay.

In vivo Tumorigenicity Assay

The animal experiments were conducted with the approval of the Animal Welfare Committee of the Third Affiliated Hospital of Chongqing Medical University (AWC. TAHCMU-2018.0216) and conformed to the NIH guidelines for the care and use of laboratory animals. The lentiviruses carrying short-hairpin RNAs (shRNAs) against UBA6-AS1 (sh-UBA6-AS1) and NC shRNA (sh-NC) were prepared by Shanghai GenePharma, Co., Ltd. U251 cells were transfected with the lentiviruses, and puromycin was employed for selecting U251 cells with stable UBA6-AS1 silencing. For xenograft experiments, male BALB/c nude mice, aged 4 weeks and weighing 20g, were purchased from Beijing Vital River Laboratory Animal Technology Co., Ltd. The mice were subcutaneously injected with U251 cells with stable UBA6-AS1

knockdown. The size of the subcutaneous tumors was monitored weekly for 4 weeks, and their volume was calculated using the formula: Volume = 0.5 x width^2 x length. At the last observation, all mice were euthanized, and the xenograft tumors were resected, weighed and further examined.

Bioinformatics Analysis

The potential miRNAs targeting UBA6-AS1 were predicted with the application of Starbase 3.0 (http://starbase.sysu.edu.cn/) and miRDB (http://mirdb.org/). Two databases for microRNA target prediction, including TargetScan human 7.0 (http://www.targetscan.org/vert_60/) and miRDB, were used to identify the potential target of miR-760.

Nucleus-Cytoplasm Fractionation

The Cytoplasmic & Nuclear RNA Purification Kit (Norgen Biotek Corp.) was used to separate the nuclear and cytosolic fractions of GBM cells. RT-qPCR analysis was then performed to assess the subcellular location of UBA6-AS1. GAPDH served as the cytoplasm control, while U6 was used as the nuclear control.

RNA Immunoprecipitation (RIP) Assay

A Magna RIP RNA-Binding Protein Immunoprecipitation Kit (EMD Millipore) was applied in RIP assay. Briefly, GBM cell suspension was obtained by incubation with RIP buffer (Beyotime Institute of Biotechnology). Subsequently, the cell suspension was cultured with magnetic beads pre-incubated with human anti-Ago2 antibody or normal mouse IgG (EMD Millipore). Following overnight incubation at 4°C, the magnetic beads were harvested and treated with Proteinase K for protein digestion. The precipitated RNA was extracted and analyzed by RT-qPCR to detect the enrichment of UBA6-AS1 and miR-760.

RNA Pull-Down Assay

The direct binding interaction between UBA6-AS1 and miR-760 in GBM cells was further uncovered by RNA pull-down assay. A Pierce™ Biotin 3′ End DNA Labeling Kit (Thermo Fisher Scientific, Inc.) was employed for preparing the biotinylated RNA. GBM cells were transfected with biotinylated miR-760 mimic (bio-miR- miR-760) or biotinylated miR-NC (bio-miR-NC) utilizing Lipofectamine™ 2000 reagent. Forty-eight hours later, the transfected cells were harvested and cultivated with pre-cooled lysis buffer. Subsequent to centrifugation, the supernatant was incubated with Dynabeads M-280 Streptavidin (BD Biosciences) at 4°C for 2 h, yielding the g bio-miRNA-lncRNA complexes. At last, the relative enrichment of UBA6-AS1 and miR-760 in the formed complexes was examined via performing RT-qPCR.

Luciferase Reporter Assay

The fragments of UBA6-AS1 and HOXA2 3′-UTR carrying the wild-type (wt) miR-760-binding sequences were amplified and inserted into the pMIR-luciferase reporter plasmid (Promega Corporation) to construct the UBA6-AS1-wt and HOXA2-wt luciferase reporter vectors. The corresponding mutant (mut) binding sequences were obtained by QuikChange site-directed mutagenesis kit (Stratagene; Agilent Technologies, Inc.), and the mutant fragments were also cloned into the pMIR-luciferase reporter plasmid to generate the reporter vectors UBA6-AS1-mut and HOXA2-mut. For the luciferase reporter assay, GBM cells were seeded into 24-well plates one night prior to transfection. Cells were pre-transfected with miR-760 mimic or miR-NC, followed by another transfection of generated reporter vectors. Two days later, the luciferase activity was tested using the Dual-Luciferase report assay system (Promega Corporation).

Western Blotting

Proteins were isolated from transfected cells using RIPA Lysis Buffer (KeyGen BioTECH). A BCA Protein Assay Kit (KeyGen BioTECH) was utilized for protein sample quantification. Equal amounts of protein were subjected to 10% SDS-PAGE and transferred to PVDF membranes. After blocking at room temperature for 2 h with 5% skimmed milk, the membranes were probed with the primary antibodies targeting HOXA2 (ab229960; dilution 1:1000; Abcam) or GAPDH (ab181602; dilution 1:1000; Abcam). Thereafter, goat anti-rabbit HRP (IgG) secondary antibody (ab205718; dilution 1:5000; Abcam) was incubated with the membranes at room temperature for 2 h. Visualization was performed using the ECL Substrate (KeyGen BioTECH). GAPDH served as the loading control.

Statistical Analysis

All results are presented as the mean ± standard deviation from at least 3 independent experiments. The difference

between two groups was compared with Student's *t*-test. One-way analysis of variance with Tukey's post hoc test was used for examining differences among multiple groups. The overall survival of patients with GBM was analyzed by the Kaplan-Meier method and compared with the Log rank test. The correlation of the expression of UBA6-AS1 with miR-760 and HOXA2 was examined using Pearson's correlation analysis. All statistical analyses were performed using SPSS 21.0 (IBM Corp.) and P<0.05 was considered to indicate a statistically significant difference.

Results

Interference of UBA6-AS1 Restricts Cell Proliferation, Migration and Invasion and Promotes Cell Apoptosis in GBM

To investigate the function of UBA6-AS1 in GBM, its expression in GBM was initially analyzed using TCGA database. High UBA6-AS1 expression was observed in GBM in contrast to that in normal tissues (Figure 1A). To confirm this finding, RT-qPCR analysis was performed to measure UBA6-AS1 expressi[illegible] GBM tissues. As

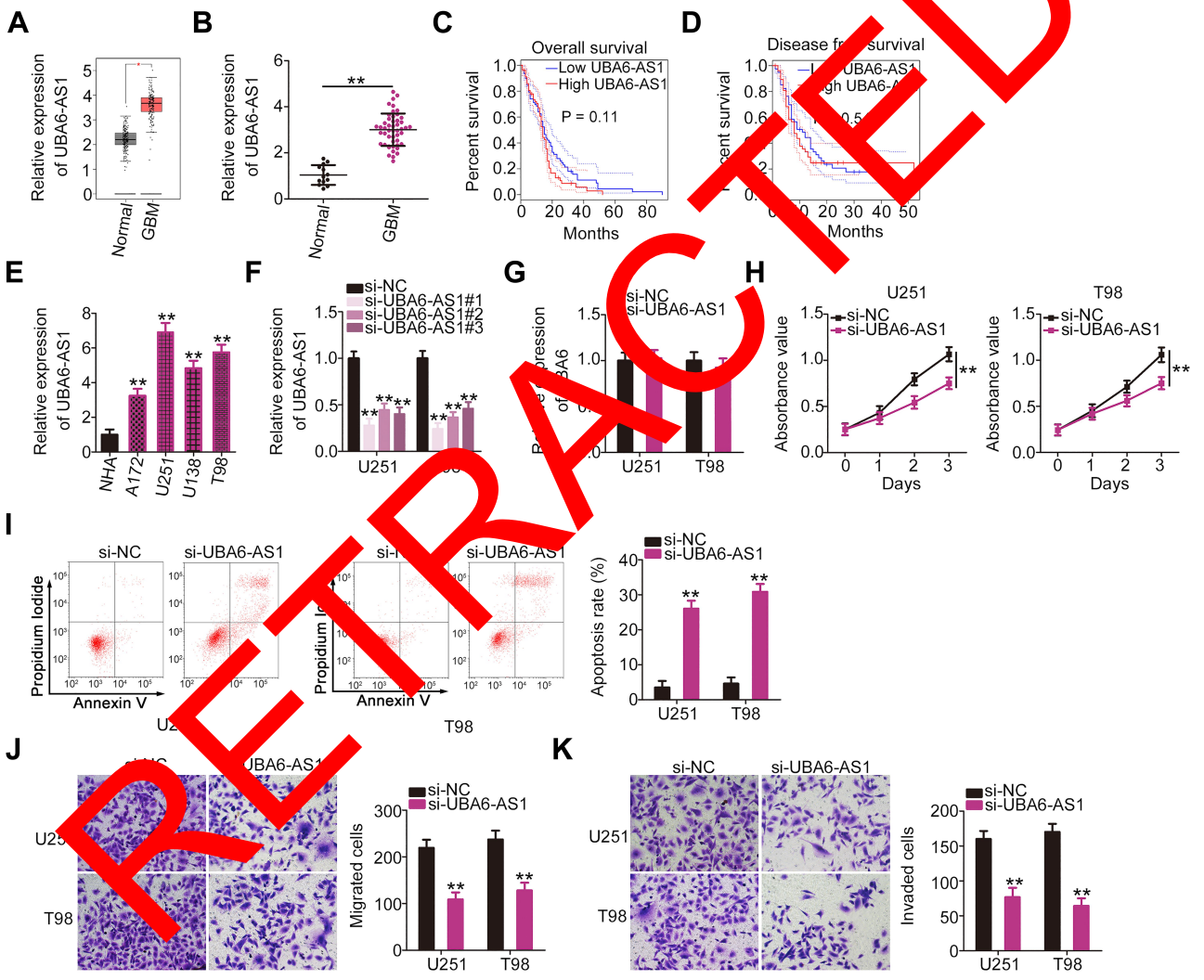

Figure 1 UBA6-AS1 plays an oncogenic role in GBM. (**A**) UBA6-AS1 expression in GBM was analyzed using TCGA database. (**B**) RT-qPCR analysis was conducted to detect UBA6-AS1 expression in 49 GBM tissues and 13 normal brain tissue samples. (**C**, **D**) TCGA database was employed to determine the association between UBA6-AS1 expression and overall survival or disease-free survival in GBM. (**E**) The expression level of UBA6-AS1 in a panel of GBM cell lines (A172, U251, U138 and T98) was measured by RT-qPCR, with a normal human astrocyte cell line NHA as the control. (**F**) Transfection efficiency of si-UBA6-AS1#1, si-UBA6-AS1#2, and si-UBA6-AS1#3 in U251 and T98 cells was evaluated by RT-qPCR analysis. (**G**) RT-qPCR was conducted to measure UBA6 expression in U251 and T98 cells after si-UBA6-AS1 or si-NC transfection. (**H**) U251 and T98 cells with UBA6-AS1 silencing were subjected to Cell Counting Kit-8 assay to evaluate cell proliferation. (**I**) The effect of si-UBA6-AS1 on U251 and T98 cell apoptosis was assessed by flow cytometric analysis. (**J**, **K**) Transwell migration and invasion assays were used to determine the migration and invasion abilities of U251 and T98 cells following si-UBA6-AS1 or si-NC transfection. *P < 0.05 and **P < 0.01.

Abbreviations: GBM, glioblastoma; RT-qPCR, reverse transcription-quantitative PCR; TCGA, The Cancer Genome Atlas; UBA6-AS1, UBA6 antisense RNA 1; si-NC, negative control small interfering RNA; si-UBA6-AS1, small interfering RNA targeting UBA6-AS1.

compared with normal brain tissues, UBA6-AS1 was markedly overexpressed in GBM tissues (Figure 1B). Subsequently, the correlation between UBA6-AS1 expression and overall or disease-free survival in patients with GBM was investigated using TCGA database. The upregulated UBA6-AS1 expression was not found to be associated with either overall survival (Figure 1C) or disease-free survival (Figure 1D) in patients with GBM.

As mentioned, an increased level of UBA6-AS1 in GBM was identified in both TCGA database and our sample cohort. Thus, UBA6-AS1 may act as a regulator of GBM progression. First, the expression level of UBA6-AS1 in GBM cell lines was detected using RT-qPCR. The UBA6-AS1 level was notably higher in GBM cell lines (A172, U251, U138 and T98) compared with that in NHA cells (Figure 1E). UBA6-AS1 expression was downregulated in the U251 and T98 cell lines by si-UBA6-AS1 transfection. UBA6-AS1 knockdown in si-UBA6-AS1-transfected U251 and T98 cells was confirmed by RT-qPCR analysis (Figure 1F). The si-UBA6-AS1#1 was used in subsequent experiments considering its superior efficacy in silencing UBA6-AS1 expression. To investigate whether si-UBA6-AS1 can disturb UBA6, UBA6 expression in UBA6-AS1-silenced GBM cells was determined utilizing RT-qPCR. The data verified that transfection with si-UBA6-AS1 did not affect UBA6 expression in GBM cells (Figure 1G). The data of the CCK-8 assay revealed suppressed proliferation in UBA6-AS1-knockdown U251 and T98 cells in comparison with that in cells transfected with si-NC (Figure 1H). As evidenced by flow cytometric analysis, knockdown of UBA6-AS1 enhanced the apoptosis of U251 and T98 cells (Figure 1I). Furthermore, both cell migration (Figure 1J) and invasion (Figure 1K) of U251 and T98 cells were decreased by UBA6-AS1 silencing. These findings demonstrated that UBA6-AS1 plays an oncogenic role during GBM progression.

UBA6-AS1 Sponges miR-760 in GBM Cells

To elucidate the mechanism underlying the role of UBA6-AS1 in GBM, its subcellular distribution was predicted via lncLocator (http://www.csbio.sjtu.edu.cn/bioinf/lncLocator/). UBA6-AS1 was found to be enriched in the cytoplasm (Figure 2A). Nucleus-cytoplasm fractionation assay also confirmed UBA6-AS1 as a cytoplasmic lncRNA in GBM cells (Figure 2B). Accordingly, it was hypothesized that UBA6-AS1 may function as a ceRNA in GBM. The ENCORI and miRDB databases were utilized to screen for potential target miRNAs of UBA6-AS1. A total of 10 miRNAs were predicted as potential miRNAs sequestered by UBA6-AS1 (Figure 2C). Then, RT-qPCR was conducted to measure the expression of miR-378a-3p, miR-378b/c/d/e/f/h/I, miR-422a and miR-760 in U251 and T98 cells following UBA6-AS1 knockdown. miR-760 was upregulated in U251 and T98 cells with UBA6-AS1 silencing, whereas the expression of other miRNAs was unaffected in response to si-UBA6-AS1 transfection (Figure 2D). To explore whether UBA6-AS1 expression can be influenced by miR-760, RT-qPCR was done to determine UBA6-AS1 expression in miR-760-overexpressed U251 and T98 cells. The data confirmed that enforced miR-760 expression did not affect the expression of UBA6-AS1 in U251 and T98 cells (Figure 2E). Additionally, miR-760 was found to be downregulated in GBM tissues compared with normal brain tissues (Figure 2F). Furthermore, Pearson's correlation analysis verified that the expression of miR-760 was inversely associated with UBA6-AS1 expression in GBM tissues (Figure 2G).

To further validate the binding between miR-760 and UBA6-AS1 (Figure 2H), luciferase reporter assay was carried out in U251 and T98 cells following co-transfection with miR-760 mimic or miR-NC and UBA6-AS1-wt or UBA6-AS1-mut. The results revealed that upregulation of miR-760 lowered the luciferase activity of UBA6-AS1-wt in U251 and T98 cells, whereas the two cell lines co-transfected with miR-760 mimic and UBA6-AS1-mut manifested no change of luciferase activity (Figure 2I). In addition, the RIP assay confirmed that miR-760 and UBA6-AS1 could be enriched by Ago2 (Figure 2J), suggesting that miR-760 and UBA6-AS1 could be recruited to the same RNA-induced silencing complexes. Besides, RNA pull-down assay uncovered that relative UBA6-AS1 enrichment was higher in the bio-miR-760 group than in bio-miR-NC group, further confirming that UBA6-AS1 bound to miR-760 (Figure 2K). Taken together, these findings indicate that UBA6-AS1 may directly target miR-760 in GBM cells as a molecular sponge.

miR-760 Overexpression Suppresses the Aggressive Phenotype of GBM Cells

miR-760 expression was also detected in a panel of GBM cell lines. As compared with NHA cells, miR-760 was

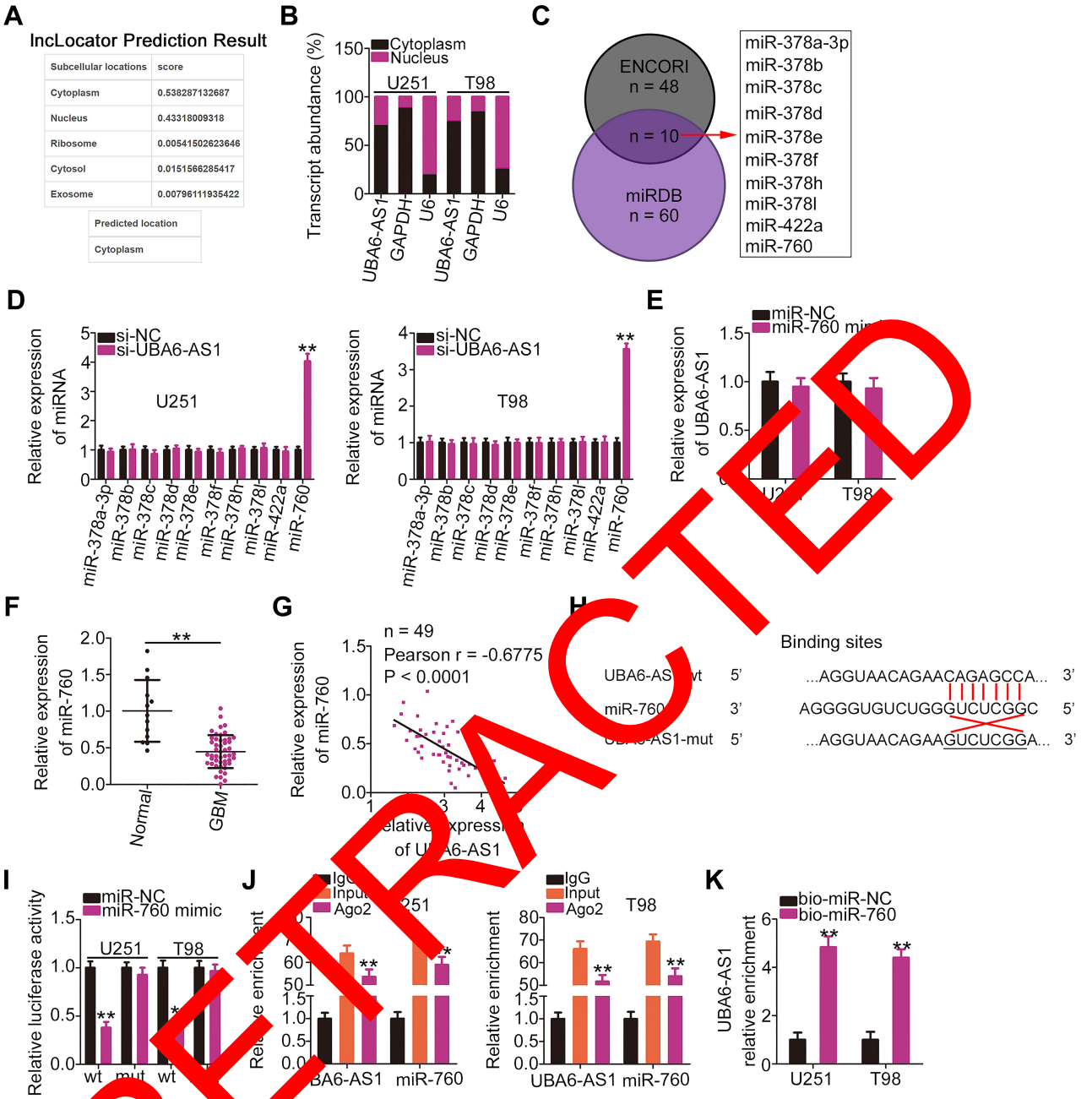

Figure 2 UBA6-AS1 acts as a molecular sponge for miR-760 in GBM cells. (**A**) The localization of UBA6-AS1 was predicted by lncLocator. (**B**) Nucleus-cytoplasm fractionation assay was used to determine the subcellular distribution of UBA6-AS1 in U251 and T98 cells. (**C**) The potential miRNAs targeting UBA6-AS1 were predicted by the ENCORI and miRDB databases. (**D**) The expression of miRNAs (miR-378a-3p, miR-378b/c/d/e/f/h/l, miR-422a and miR-760) was detected in UBA6-AS1-depleted U251 and T98 cells via RT-qPCR analysis. (**E**) RT-qPCR was implemented to measure UBA6-AS1 expression in miR-760 mimic-transfected or miR-NC-transfected U251 and T98 cells. (**F**) miR-760 expression in 49 GBM tissues and 13 normal brain tissue samples was analyzed by RT-qPCR. (**G**) Pearson's correlation analysis was used to determine the correlation between the expression of miR-760 and that of UBA6-AS1 in 49 GBM tissues. (**H**) Wild-type and mutant binding sites between miR-760 and UBA6-AS1. (**I**) Luciferase reporter gene assay was conducted to confirm the targeting association between miR-760 and UBA6-AS1. Luciferase activity was measured in U251 and T98 cells transfected with miR-760 mimic or miR-NC in combination with UBA6-AS1-wt or UBA6-AS1-mut. (**J**) Radioimmunoprecipitation assays revealed Ago2 antibody enrichment of miR-760 and UBA6-AS1 in U251 and T98 cells. (**K**) U251 and T98 cells were transfected with bio-miR-760 and bio-miR-NC. After transfection, RT-qPCR was performed to assess the relative enrichment of UBA6-AS1 in the formed bio-miRNA-lncRNA complexes. **P < 0.01.

Abbreviations: GBM, glioblastoma; RT-qPCR, reverse transcription-quantitative PCR; miR-NC, negative control miRNA mimic; miR, microRNA; UBA6-AS1, UBA6 antisense RNA 1; si-NC, negative control small interfering RNA; si-UBA6-AS1, small interfering RNA targeting UBA6-AS1; wt, wild-type; mut, mutant; Ago2, Argonaute 2.

downregulated in all four examined GBM cell lines (Figure 3A). The miR-760 overexpression in U251 and T98 cells was detected when miR-760 mimic was introduced into the cells (Figure 3B). The effects of miR-760 upregulation on the proliferation and apoptosis of GBM cells were determined by CCK-8 assay and flow cytometric analysis,

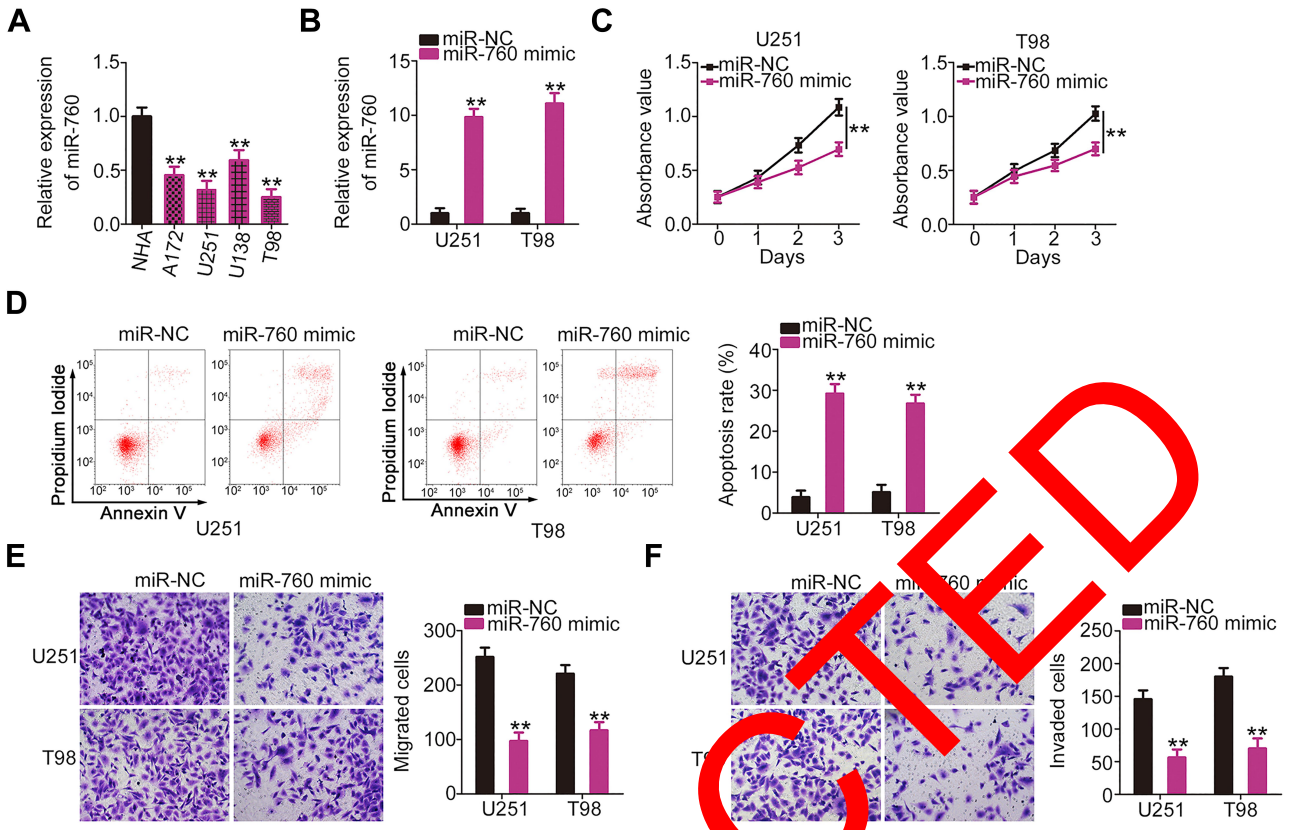

Figure 3 Ectopic miR-760 expression inhibits the growth and invasion of GBM in vitro. (**A**) miR-760 expression in GBM cell lines (A172, U251, U138 and T98) and a normal human astrocyte cell line (NHA) was detected by RT-qPCR analysis. (**B**) U251 and T98 cells transfected with miR-760 mimic or miR-NC were harvested and analyzed with RT-qPCR to evaluate the transfection efficiency of miR-760 mimic. (**C**, **D**) Cell Counting Kit-8 assay and flow cytometric analysis were conducted to determine the proliferation and apoptosis of miR-760-overexpressing U251 and T98 cells, respectively. (**E**, **F**) The migration and invasion of U251 and T98 cells with miR-760 mimic or miR-NC transfection were examined by Transwell assays. **P < 0.

Abbreviations: GBM, glioblastoma; RT-qPCR, reverse transcription-quantitative PCR; miR-NC, negative control miRNA mimic; miR, microRNA.

respectively. Ectopic miR-760 expression suppressed the proliferation (Figure 3C) and promoted the apoptosis (Figure 3D) of U251 and T98 cells. Furthermore, the number of migrating (Figure 3E) and invading (Figure 3F) U251 and T98 cells was significantly decreased following transfection with miR-760 mimic. These results confirmed miR-760 as an anti-oncogenic miRNA in GBM cells.

UBA6-AS1 Upregulates HOXA2 in GBM Cells by Sequestering miR-760

Through bioinformatics analysis, the HOXA2 3′-UTR was found to have a putative binding site for miR-760 (Figure 4A). To verify this prediction, RT-qPCR analysis and Western blotting were employed to determine whether miR-760 exerts regulatory effects on HOXA2 expression. Notably, the mRNA (Figure 4B) and protein (Figure 4C) levels of HOXA2 were decreased in U251 and T98 cells that were transfected with miR-760 mimic. In addition, HOXA2 expression was increased in GBM tissues compared with normal brain tissues (Figure 4D), exhibiting an inverse expression pattern with miR-760 (Figure 4E). Luciferase reporter assay was then performed, and the results indicated that the luciferase activity of HOXA2-wt was markedly inhibited by miR-760 mimic in U251 and T98 cells, while the activity of HOXA2-mut exhibited no obvious change following miR-760 overexpression (Figure 4F).

HOXA2 was identified as direct target of miR-760 in GBM cells. Thus, it was next attempted to explore the association among UBA6-AS1, miR-760 and HOXA2 expression in GBM. First, Pearson's correlation analysis uncovered a notable positive correlation between UBA6-AS1 and HOXA2 expression in GBM tissues (Figure 4G). Furthermore, loss of UBA6-AS1 suppressed HOXA2 mRNA (Figure 4H) and protein (Figure 4I) expression in U251 and T98 cells, which was partially recovered by miR-760 inhibitor (Figure 4J and K). Finally, RIP assay demonstrated that

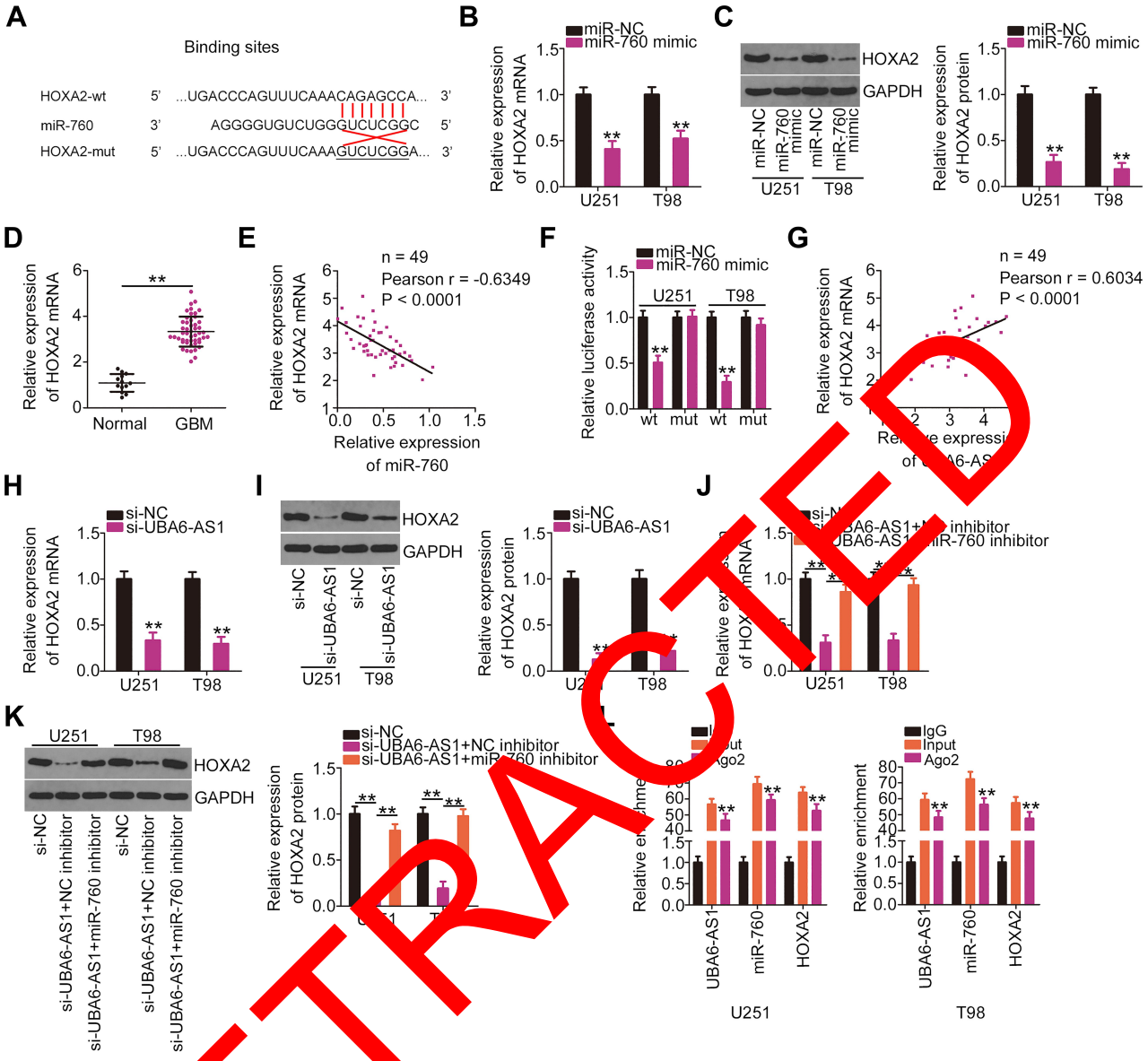

Figure 4 UBA6-AS1 increases the expression of HOXA2 in GBM cells by sponging miR-760. (**A**) Wild-type and mutant binding sites between miR-760 and the 3′-untranslated region of HOXA2. (**B**) The mRNA and protein levels of HOXA2 in U251 and T98 cells transfected with miR-760 mimic or miR-NC were determined by RT-qPCR analysis and Western blotting, respectively. (**D**) HOXA2 mRNA in 49 GBM tissues and 13 normal brain tissues was detected by RT-qPCR analysis. (**E**) Pearson's correlation analysis of miR-760 and HOXA2 mRNA levels in the 49 GBM tissues. (**F**) Luciferase reporter assay was employed to measure the luciferase activity of U251 and T98 cells following co-transfection with miR-760 mimic or miR-NC and HOXA2-wt or HOXA2-mut. (**G**) The correlation between the levels of HOXA2 mRNA and UBA6-AS1 in the 49 GBM tissue samples was tested by Pearson's correlation analysis. (**H**, **I**) RT-qPCR analysis and Western blotting were used to determine HOXA2 mRNA and protein levels in U251 and T98 cells transfected with si-UBA6-AS1 or si-NC. (**J**, **K**) U251 and T98 cells were transfected with miR-760 inhibitor or NC inhibitor along with si-UBA6-AS1. The mRNA and protein levels of HOXA2 were determined by RT-qPCR analysis and Western blotting, respectively. (**L**) Radioimmunoprecipitation assay was performed with IgG and Ago2 antibody, followed by RT-qPCR analysis of UBA6-AS1, miR-760 and HOXA2 enrichment. **P < 0.01.

Abbreviations: GBM, glioblastoma; RT-qPCR, reverse transcription-quantitative PCR; HOXA2, homeobox A2; wt, wild-type; mut, mutant; Ago2, Argonaute 2; GAPDH, glyceraldehyde-3-phosphate dehydrogenase; miR, microRNA; miR-NC, negative control miRNA mimic; UBA6-AS1, UBA6 antisense RNA 1; si-NC, negative control small interfering RNA; si-UBA6-AS1, small interfering RNA targeting UBA6-AS1; NC inhibitor, negative control inhibitor.

UBA6-AS1, miR-760 and HOXA2 were all immunoprecipitated by Ago2 (Figure 4L). Collectively, these findings demonstrated that UBA6-AS1 acts as a ceRNA in GBM cells by sponging miR-760 and, consequently, enhancing HOXA2 expression.

miR-760 Inhibitor or HOXA2 Restoration Offsets the Impacts of Si-UBA6-AS1 on the Tumor Phenotypes of GBM Cells

Rescue experiments were employed to elucidate whether the pro-oncogenic effects of UBA6-AS1 on GBM cells

were mediated through targeting the miR-760/HOXA2 axis. miR-760 inhibitor was used in the assay, and RT-qPCR analysis confirmed that transfection of miR-760 inhibitor resulted in significant downregulation of miR-760 in both U251 and T98 cells (Figure 5A). In the CCK-8 assay, the proliferation of U251 and T98 cells was markedly inhibited following UBA6-AS1 knockdown, and was then abolished by miR-760 inhibition (Figure 5B). Additionally, flow cytometric analysis revealed that depletion of UBA6-AS1 promoted the apoptosis of U251 and T98 cells, while this effect was significantly counteracted by miR-760 inhibitor co-transfection (Figure 5C). Furthermore, the inhibition of the migration (Figure 5D) and invasion (Figure 5E) of U251 and T98 cells induced by si-UBA6-AS1 could be rescued by miR-760 downregulation.

Subsequently, HOXA2 overexpression plasmid pcDNA3.1-HOXA2 was also used, and its efficiency in upregulating HOXA2 expression was confirmed by Western blotting (Figure 6A). The si-UBA6-AS1-induced decrease in cell proliferation was recovered upon reintroduction of HOXA2 (Figure 6B). Furthermore, the effects of UBA6-AS1 silencing on the apoptosis (Figure 6C), migration and invasion (Figure 6D) of U251 and T98 cells were reversed by HOXA2 overexpression. In summary, UBA6-AS1 promoted the malignancy of GBM cells by targeting miR-760/HOXA2.

UBA6-AS1 Depletion Decreases GBM Growth in vivo

The effects of UBA6-AS1 on the growth of GBM in vivo were investigated by an in vivo tumorigenicity assay. The tumor growth was slower (Figure 7A and B), and the tumor weight was lower (Figure 7C) in the sh-UBA6-AS1 group compared with those in the sh-NC group. The tumor xenografts were removed at the end of the assay and used to measure the expression of UBA6-AS1, miR-760 and HOXA2. The results revealed that the tumor xenografts in the sh-UBA6-AS1 group exhibited lower UBA6-AS1 (Figure 7D) and HOXA2 protein (Figure 7E), as well as higher miR-760 expression (Figure 7F) compared with the sh-NC group. Collectively, these findings indicated that inhibition of UBA6-AS1 impaired the growth of GBM in vivo.

Discussion

A large number of lncRNAs are aberrantly expressed in GBM and have been identified as critical regulatory factors in oncogenesis and progression.[26,27] LncRNAs may function as promoters or inhibitors of cancer-associated genes in GBM, and have the ability to modulate the aggressive tumor phenotypes.[28,29] Accordingly, lncRNAs appear to be promising molecular targets for GBM therapy. With the advances in sequencing technologies, numerous lncRNAs have been identified in the human genome;[30,31] however, the biological roles and underlying mechanisms of the majority of lncRNAs in GBM have not been extensively investigated. Thus, the aim of the present study was to investigate in detail the role of UBA6-AS1 in the modulation of the malignant properties of GBM and explore the possible underlying mechanism.

The expression pattern of UBA6-AS1 in GBM was initially examined. Of note, the data revealed that UBA6-AS1 was overexpressed in GBM, which was consistent with the data from TCGA database. After silencing UBA6-AS1, the specific functions of UBA6-AS1 in GBM cells in vitro and in vivo were comprehensively determined through a series of functional experiments. The results demonstrated that UBA6-AS1 exerted tumor-promoting effects on GBM. Upon UBA6-AS1 knockdown, GBM cell proliferation, migration and invasion were obviously decreased and cell apoptosis was enhanced in vitro. Furthermore, depletion of UBA6-AS1 suppressed the growth of GBM in vivo. To the best of our knowledge, the results of the present study are the first to verify that UBA6-AS1 functions as a pro-oncogenic lncRNA in GBM, and it may represent a possible target for GBM treatment.

The molecular events through which lncRNAs exert their effects are complicated and are largely determined by their subcellular distribution.[32] The lncRNAs located in the nucleus may interact with the epigenetic modification complex and affect chromatin architecture, consequently regulating genes at the transcriptional level.[33] As regards cytoplasmic lncRNAs, the ceRNA theory, first proposed by Salmena et al, has received extensive attention and has been widely acknowledged.[34] LncRNAs may act as ceRNAs to sequester miRNAs by sharing common miRNA response elements, so as to restrict or decrease the control of miRNAs on target genes.[35]

We next sought to identify the mechanism of action of UBA6-AS1 in GBM in the present study. By using lncRNA subcellular localization predictor (lncLocator) and nucleus-cytoplasm fractionation assay, UBA6-AS1 was demonstrated to be mostly distributed in the cytoplasm of GBM

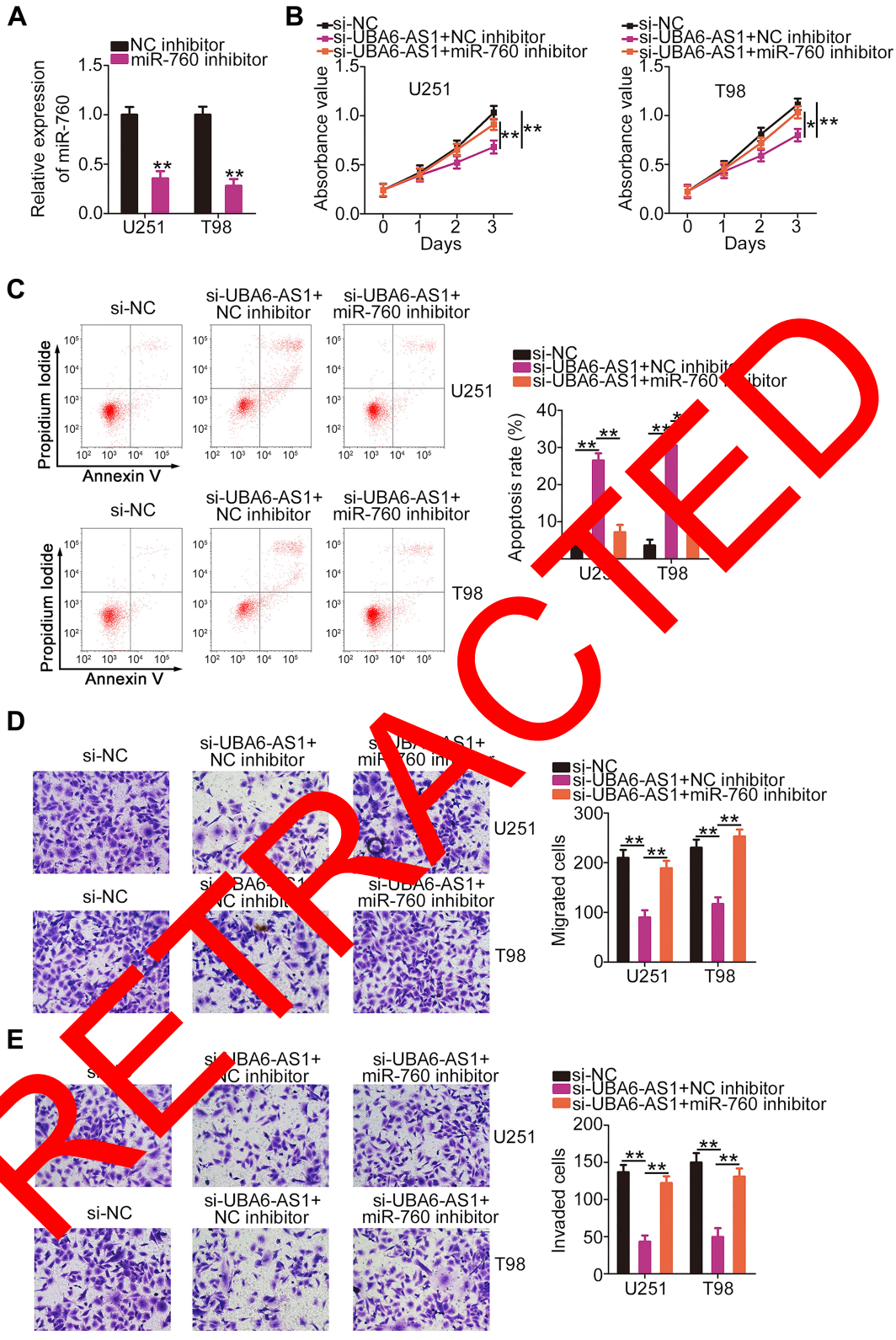

Figure 5 Inhibition of miR-760 eliminates the effects of si-UBA6-AS1 on the proliferation, apoptosis, migration and invasion of GBM cells. (**A**) Reverse transcription-quantitative PCR analysis was used to measure the expression of miR-760 in U251 and T98 cells following miR-760 inhibitor or NC inhibitor transfection. (**B**, **C**) miR-760 inhibitor or NC inhibitor along with si-UBA6-AS1 were transfected into U251 and T98 cells. The proliferation and apoptosis of co-transfected cells were assessed by Cell Counting Kit-8 assay and flow cytometric analysis, respectively. (**D**, **E**) Transwell migration and invasion assays were used to evaluate the migration and invasion abilities of U251 and T98 cells treated as described above. *P < 0.05 and **P < 0.01.

Abbreviations: GBM, glioblastoma; NC inhibitor, negative control inhibitor; UBA6-AS1, UBA6 antisense RNA 1; si-NC, negative control small interfering RNA; si-UBA6-AS1, small interfering RNA targeting UBA6-AS1.

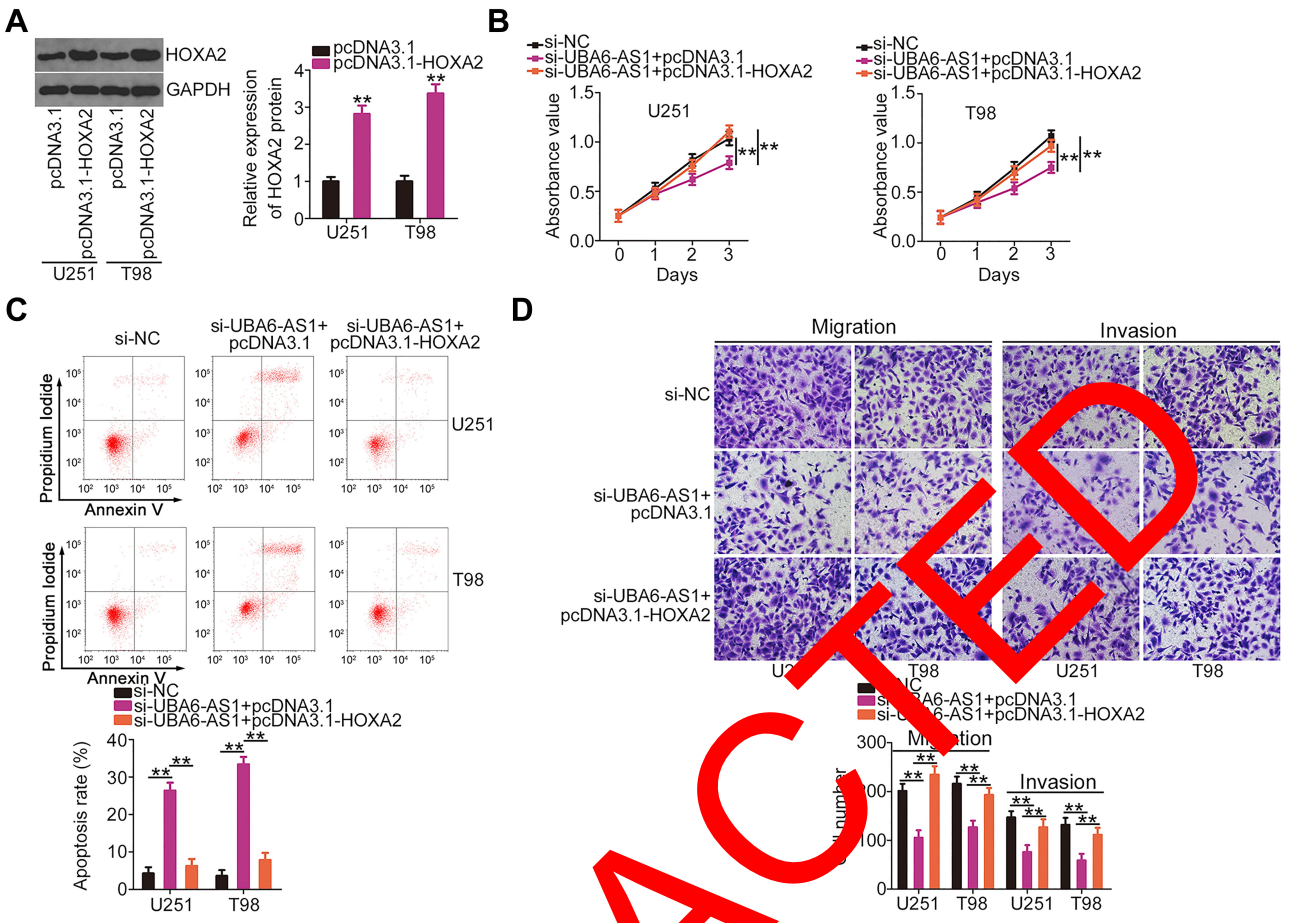

Figure 6 The UBA6-AS1 silencing-induced effects on GBM cells were weakened following HOXA2 upregulation. (**A**) Western blotting was employed to measure HOXA2 protein expression in pcDNA3.1-HOXA2-transfected or si-NC-transfected U251 and T98 cells. (**B**, **C**) Cell Counting Kit-8 assay and flow cytometric analysis were used to evaluate the proliferation and apoptosis of U251 and T98 cells following co-transfection with pcDNA3.1-HOXA2 or pcDNA3.1 and si-UBA6-AS1. (**D**) Changes in the migration and invasion of U251 and T98 cells following transfection with pcDNA3.1-HOXA2 or pcDNA3.1 in combination with si-UBA6-AS1. **P < 0.01.

Abbreviations: GBM, glioblastoma; HOXA2, homeobox A2; GAPDH, glyceraldehyde-3-phosphate dehydrogenase; UBA6-AS1, UBA6 antisense RNA 1; si-NC, negative control small interfering RNA; si-UBA6-AS1, small interfering RNA targeting UBA6-AS1.

cells, which provided a theoretical basis for UBA6-AS1 acting as a ceRNA or molecular sponge. Through bioinformatics analysis, miR-760 was predicted as the downstream miRNA of UBA6-AS1, and the prediction was subsequently verified by correlation analysis, luciferase reporter assay and RIP assay. Further mechanism investigation was implemented to identify the target of miR-760. The results indicated that miR-760 directly targeted HOXA2 and negatively regulated its expression in GBM cells. Subsequent analysis further revealed that the si-UBA6-AS1-mediated decrease in HOXA2 expression was largely rescued in GBM cells by decoying miR-760. Taken together, these findings suggested that UBA6-AS1 may serve as a ceRNA in GBM cells by sponging miR-760 to upregulate HOXA2.

As regards miR-760, it has been found to be differentially expressed in multiple human cancers and contribute to cancer progression.[36–38] However, the exact function of miR-760 in GBM remains elusive. In the present study, it was observed that miR-760 was expressed at low levels in GBM tissues and cell lines. Functionally, miR-760 overexpression effectively suppressed the malignant characteristics of GBM cells. HOXA2, a member of the HOXA cluster, was confirmed as a direct target of miR-760 in GBM cells. It was reported to be highly expressed in GBM and was positively correlated with the clinical grade, histological type, patient age and tumor recurrence.[39] In this study, the data supported that HOXA2 was regulated by the UBA6-AS1/miR-760 axis in GBM cells. Eventually, rescue experiments demonstrated that inhibition of miR-760 or overexpression of HOXA2 notably offset the effects of UBA6-AS1 silencing on GBM cells. Therefore, our results provided sufficient evidence to

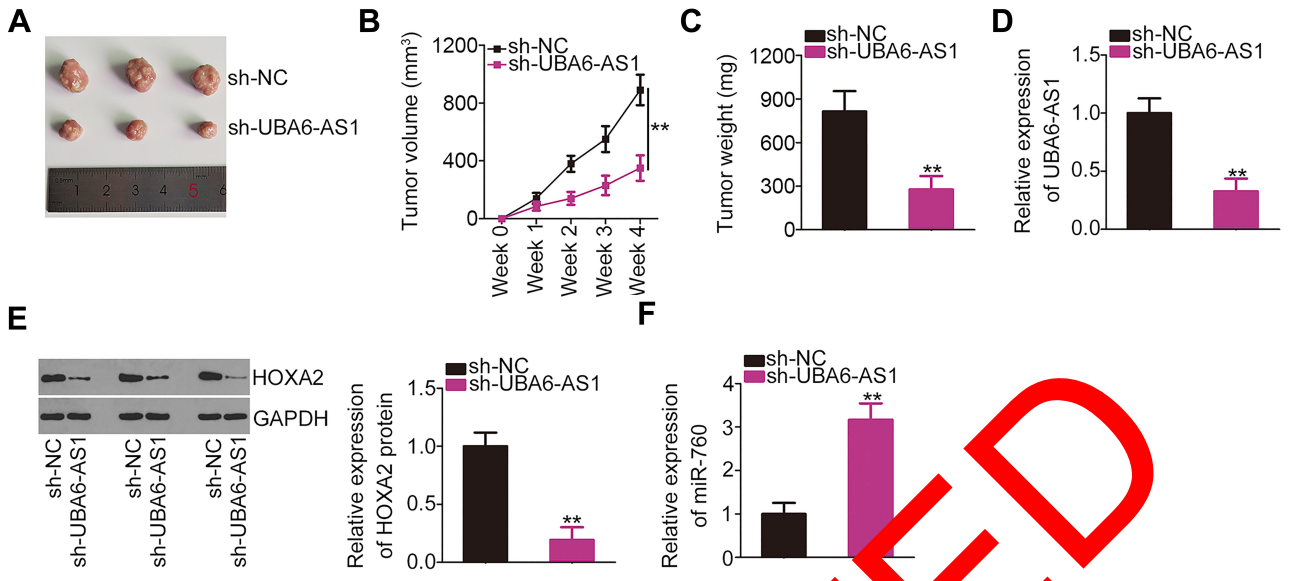

Figure 7 UBA6-AS1 depletion inhibits GBM growth in vivo. (**A**) Representative images of tumor xenografts harvested from the sh-UBA6-AS1 and sh-NC groups. (**B**) Tumor growth curves were generated according to the tumor volumes monitored weekly for 4 weeks. (**C**) The weight of the tumor xenografts dissected from the sh-UBA6-AS1 and sh-NC groups was determined. (**D**) RT-qPCR analysis was used to measure UBA6-AS1 expression in the tumor xenografts from the sh-UBA6-AS1 and sh-NC groups. (**E**) HOXA2 protein expression in tumor xenografts from the sh-UBA6-AS1 and sh-NC groups was measured by Western blotting. (**F**) RT-qPCR analysis was used to measure miR-760 expression in tumor xenografts from the sh-UBA6-AS1 and sh-NC groups. $^{**}P < 0.01$.

Abbreviations: GBM, glioblastoma; RT-qPCR, reverse transcription-quantitative PCR; HOXA2, homeobox A2; UBA6-AS1, UBA6 antisense RNA 1; sh-NC, negative control short-hairpin RNA; sh-UBA6-AS1, short-hairpin RNA targeting UBA6-AS1; GAPDH, glyceraldehyde-3-phosphate dehydrogenase; miR, microRNA.

verify that UBA6-AS1 exerts its tumor-promoting effects by sponging miR-760.

Our study had two limitations. Firstly, only 49 GBM tissues and 13 normal brain tissues were used to detect UBA6-AS1, miR-760 and HOXA2 expression. The sample size is low. Secondly, the effect of UBA6-AS1 on metastasis of GBM cells in vivo was not examined. We will resolve the two limitations in the near future. More importantly, the next steps of our study will explore the detailed mechanisms underlying the dysregulation of the UBA6-AS1 in GBM.

Conclusion

In summary, UBA6-AS1 was found to be overexpressed in GBM tissues and cell lines. UBA6-AS1 interference markedly suppressed the oncogenicity of GBM cells by inhibiting their proliferation, migration and invasion and promoting their apoptosis. Mechanistically, UBA6-AS1 may function as a ceRNA by sponging miR-760 and consequently enhancing HOXA2 expression. The newly identified UBA6-AS1/miR-760/HOXA2 axis may be of value as a target in the treatment of GBM.

Disclosure

All the authors declare that they have no competing interests.

References

1. Louis DN, Perry A, Reifenberger G, et al. The 2016 World Health Organization classification of tumors of the central nervous system: a summary. *Acta Neuropathol*. 2016;131(6):803–820. doi:10.1007/s00401-016-1545-1
2. Huang BS, Luo QZ, Han Y, Huang D, Tang QP, Wu LX. MiR-223/PAX6 axis regulates glioblastoma stem cell proliferation and the chemo resistance to TMZ via regulating PI3K/Akt pathway. *J Cell Biochem*. 2017;118(10):3452–3461. doi:10.1002/jcb.26003
3. Barnholtz-Sloan JS, Ostrom QT, Cote D. Epidemiology of brain tumors. *Neurol Clin*. 2018;36(3):395–419. doi:10.1016/j.ncl.2018.04.001
4. Tykocki T, Eltayeb M. Ten-year survival in glioblastoma. A systematic review. *J Clin Neurosci*. 2018;54:7–13. doi:10.1016/j.jocn.2018.05.002
5. McGranahan T, Therkelsen KE, Ahmad S, Nagpal S. Current state of immunotherapy for treatment of glioblastoma. *Curr Treat Options Oncol*. 2019;20(3):24. doi:10.1007/s11864-019-0619-4
6. Bush NAO, Chang SM, Berger MS. Current and future strategies for treatment of glioma. *Neurosurg Rev*. 2017;40(1):1–14. doi:10.1007/s10143-016-0709-8
7. Toms SA, Tapinos N. Recent advances in the treatment of gliomas - comprehensive brain tumor center. *R I Med J*. 2017;100(6):43–46.
8. Phillips RE, Soshnev AA, Allis CD. Epigenomic reprogramming as a driver of malignant glioma. *Cancer Cell*. 2020;38(5):647–660. doi:10.1016/j.ccell.2020.08.008
9. Arafa K, Emara M. Insights about circadian clock and molecular pathogenesis in gliomas. *Front Oncol*. 2020;10:199. doi:10.3389/fonc.2020.00199
10. Huarte M. The emerging role of lncRNAs in cancer. *Nat Med*. 2015;21(11):1253–1261. doi:10.1038/nm.3981
11. Maruyama R, Suzuki H. Long noncoding RNA involvement in cancer. *BMB Rep*. 2012;45(11):604–611. doi:10.5483/BMBRep.2012.45.11.227

12. Quinn JJ, Chang HY. Unique features of long non-coding RNA biogenesis and function. *Nat Rev Genet*. 2016;17(1):47–62. doi:10.1038/nrg.2015.10
13. Peng L, Jiang J, Tang B, Nice EC, Zhang YY, Xie N. Managing therapeutic resistance in breast cancer: from the lncRNAs perspective. *Theranostics*. 2020;10(23):10360–10377. doi:10.7150/thno.49922
14. Jiang W, Xia J, Xie S, et al. Long non-coding RNAs as a determinant of cancer drug resistance: towards the overcoming of chemoresistance via modulation of lncRNAs. *Drug Resist Updat*. 2020;50:100683. doi:10.1016/j.drup.2020.100683
15. Zhao J, Liu D, Yang H, Yu S, He H. Long noncoding RNAs in head and neck squamous cell carcinoma: biological functions and mechanisms. *Mol Biol Rep*. 2020;47(10):8075–8090. doi:10.1007/s11033-020-05777-w
16. Ni H, Wang K, Xie P, Zuo J, Liu W, Liu C. LncRNA SAMMSON knockdown inhibits the malignancy of glioblastoma cells by inactivation of the PI3K/Akt pathway. *Cell Mol Neurobiol*. 2020. doi:10.1007/s10571-020-00833-2
17. Luo L, Zhang Y, He H, Chen C, Zhang B, Cai M. LncRNA FEZF1-AS1 sponges miR-34a to upregulate Notch-1 in glioblastoma. *Cancer Manag Res*. 2020;12:1827–1833. doi:10.2147/CMAR.S240531
18. Liang R, Tang Y. LINC00467 knockdown repressed cell proliferation but stimulated cell apoptosis in glioblastoma via miR-339-3p/IP6K2 axis. *Cancer Biomarkers*. 2020;28(2):169–180. doi:10.3233/CBM-190939
19. Lin S, Gregory RI. MicroRNA biogenesis pathways in cancer. *Nat Rev Cancer*. 2015;15(6):321–333. doi:10.1038/nrc3932
20. Kasinski AL, Slack FJ. Epigenetics and genetics. MicroRNAs en route to the clinic: progress in validating and targeting microRNAs for cancer therapy. *Nat Rev Cancer*. 2011;11(12):849–864.
21. Weng W, Zhang Z, Huang W, et al. Identification of a compet endogenous RNA network associated with prognosis of pancrea adenocarcinoma. *Cancer Cell Int*. 2020;20(1):231. doi:10.1186 s12935-020-01243-6
22. Wu Y, Qian Z. Long non-coding RNAs (lncRNAs) mic RNAs regulatory pathways in the tumorigenesis and path enesis of oma. *Discov Med*. 2019;28(153):129–138.
23. Abdollahzadeh R, Daraei A, Mansoori Y, Se hvani moli MM, Tavakkoly-Bazzaz J. Competing endog us RNA (NA) cross talk and language in ceRNA regula etworks: a n look at hallmarks of breast cancer. *Cell Physiol*. 2019;234 (7):10080–10100. doi:10.1002/j 27941
24. Paulmurugan R, Malhotra Massoud TF. The otean world of non-coding RNAs in gli stoma. *Mol Med*. 2019;97(7):909–925. doi:10.1007/s00109-019 1798-6
25. Zeng T, Li L, Zhou Y, Ga xploring g noncoding RNAs in glioblastoma: ry m hanisms and clinical potentials. *Int J Genom*. 2018; 18:2895 :10.1155/2018/2895958
26. Xu J, Hou X, Pang L, et al. Identification of dysregulated competitive endogenous RNA networks driven by copy number variations in malignant gliomas. *Front Genet*. 2019;10:1055. doi:10.3389/fgene.2019.01055
27. Liu Q, Qi C, Li G, Su W. Prediction of the outcome for patients with glioblastoma with lncRNA expression profiles. *Biomed Res Int*. 2019;2019:5076467. doi:10.1155/2019/5076467
28. Liu G, Pan Y, Li Y, Xu H. lncRNA and mRNA signature for prognosis prediction of glioblastoma. *Future Oncol*. 2020;16(13):837–848. doi:10.2217/fon-2019-0538
29. Zhang X, Kiang KM, Zhang GP, Leung GK. Long non-coding RNAs dysregulation and function in glioblastoma stem cells. *Non-Coding RNA*. 2015;1(1):69–86. doi:10.3390/ncrna1010069
30. Li M, Long S, Hu J, Wang Z, Geng C, Ou S. Systematic identification of lncRNA-based prognostic biomarkers blastoma. *Aging*. 2019;11(21):9405–9423. doi:10.18632/ ng.102395
31. Zhao C, Gao Y, Guo R, Li H, Yang B icroarray exp ion profiles and bioinformatics analysis of mRNA cRNAs, and rcRNAs in the secondary temozolomid esistant g blastoma. *Invest New Drugs*. 2020;38(5):1227–12 . doi:10.1007/s 37 -00884-3
32. Chen LL. Linking long oncoding NA local ion and function. *Trends Biochem Sci*. 20 41(9) 761–772. doi:10.1016/j.tibs.2016.07.003
33. Zhang K, Shi Z Chang YN, H ZM HX, Hong W. The ways of action of l g no oding RNAs cytoplasm and nucleus. *Gene*. 2014;547(1):1–9. doi 1016/j.gene.2014.06.043
34. Salm Poliseno L, ay Y, Kats L, Pandolfi PP. A ceRNA hy thesis: the Rosett Stone of a hidden RNA l guage? *Cell*. 2011;146(3):353–358.
35. ziq K, Cai M Dong K, Wang P, Afrifa J, Fu S. Competitive e genous netw k of lncRNA, miRNA, and mRNA in the chemor ance gastrointestinal tract adenocarcinomas. *Biomed Pharmacother*. 2020;130:110570. doi:10.1016/j.biopha.2020.110570
36. Yu B, Shen W, Jin C, Wang L, Xi Y. Over-expression of long non-coding RNA ZEB2-AS1 may predict poor prognosis and promote the migration, invasion, and epithelial-mesenchymal transition of tumor cells in non-small cell lung cancer. *Int J Biol Markers*. 2020;35(3):29–35. doi:10.1177/1724600820938385
37. Manvati MKS, Khan J, Verma N, Dhar PK. Association of miR-760 with cancer: an overview. *Gene*. 2020;747:144648. doi:10.1016/j.gene.2020.144648
38. Liu W, Li Y, Feng S, Guan Y, Cao Y. MicroRNA-760 inhibits cell viability and migration through down-regulating BST2 in gastric cancer. *J Biochem*. 2020;168(2):159–170. doi:10.1093/jb/mvaa031
39. Liu Z, Shen F, Wang H, et al. Abnormally high expression of HOXA2 as an independent factor for poor prognosis in glioma patients. *Cell Cycle*. 2020;19(13):1632–1640. doi:10.1080/15384101.2020.1762038